Organic aerosol molecular composition and gas–particle partitioning coefficients at a Mediterranean site (Corsica)

Stéphanie Rossignol[1,2,**], Florian Couvidat[3], Caroline Rio[1,***], Sébastien Fable[1], Guillaume Grignion[4], Savelli[4], Olivier Pailly[5], Eva Leoz-Garziandia[1], Jean-Francois Doussin[2,*], Laura Chiappini[1]

1. Institut National de l'Environnement Industriel et des Risques (INERIS), 60 550 Verneuil-en-Halatte, France
2. LISA, UMR CNRS 7583, Université Paris Est Créteil et Université Paris Diderot, Institut Pierre Simon Laplace, Créteil, France
3. CEREA, Joint LaboratoryEcole des Ponts ParisTech/EDF R&D, Université Paris-Est, 77455 Marne la Vallée, France
4. Qualitair Corse, Lieu-dit Lergie RN 200, 20250 Corte, France
5. Institut National de la Recherche Agronomique (INRA), 20230 San Giuliano, Corse, France

A R T I C L E   I N F O

A B S T R A C T

Molecular speciation of atmospheric organic matter was investigated during a short summer field campaign performed in a citrus fruit field in northern Corsica (June 2011). Aimedat assessing the performance on the field of newly developed analytical protocols, this work focuses on the molecular composition of both gas and particulate phases and provides an insight into partitioning behavior of the semi-volatile oxygenated fraction. Limonene ozonolysis tracers were specifically searched for, according to gas chromatography–mass spectrometry (GC–MS) data previously recorded for smog chamber experiments. A screening of other oxygenated species present in the field atmosphere was also performed. About sixty polar molecules were positively or tentatively identified in gas and/or particle phases. These molecules comprise a wide range of branched and linear, mono and di-carbonyls (C_3–C_7), mono and di-carboxylic acids (C_3–C_{18}), and compounds bearing up to three functionalities. Among these compounds, some can be specifically attributed to limonene oxidation and others can be related to α- or β-pinene oxidation. This provides an original snapshot of the organic matter composition at a Mediterranean site in summer. Furthermore, for compounds identified and quantified in both gaseous and particulate phases, an experimental gas/particle partitioning coefficient was determined. Several volatile products, which are not expected in the particulate phase assuming thermodynamic equilibrium, were nonetheless present in significant concentrations. Hypotheses are proposed to explain these observations, such as the possible aerosol viscosity that could hinder the theoretical equilibrium to be rapidly reached.

© 2015 The Research Center for Eco-Environmental Sciences, Chinese Academy of Sciences.
Published by Elsevier B.V.

* Corresponding author.
** Present address: IRCELYON, Institut de Recherches sur la Catalyse et l'Environnement de Lyon, UMR5256, 2 Avenue Albert Einstein, 69626 Villeurbanne, France.
*** Present address: ASPA, Espace Européen de l'Entreprise de Strasbourg, 5 rue de Madrid, 67,300 Schiltigheim, France.
E-mail address: jean-francois.doussin@lisa.u-pec.fr (J.-F. Doussin).

Introduction

The formation of organic particulate matter in the earth's atmosphere through gas-to-particle transfer during atmospheric oxidation of volatile organic compounds (VOC), namely secondary organic aerosol (SOA) formation, is involved in both air quality and climate issues (IPCC 2007; Hallquist et al. 2009). However, despite substantial advances during the last decade (Donahue et al. 2006; Tsimpidi et al. 2010; Valorso et al. 2011; Couvidat et al. 2012), significant efforts are still currently provided in modeling studies to take into account the gas/particle partitioning behavior of the semi-volatile fraction of the secondary organic matter. Understanding the processes involved in these gas/particle equilibriums is indeed crucial for a better assessment of SOA yields, SOA chemical composition and thus SOA's influence on climate and health. SOA growth is usually described by absorption into the organic phase of the aerosols of semi- and non-volatile secondary species formed in the gas phase by atmospheric oxidation of precursor VOC (Odum et al. 1996; Seinfeld and Pankow 2003; Asher and Pankow 2006). Nevertheless, SOA formation and aging also involve chemical processes into the particle phase (Graber and Rudich, 2006; Healy et al. 2008; Kroll and Seinfeld, 2008; Monks et al. 2009) or at the gas–particle interface (Rudich et al. 2007, George and Abbatt 2010). This results in continuous modifications of SOA chemical composition and physico-chemical properties, influencing in turn the partitioning of the semi-volatile species (Healy et al. 2008). Such phenomena have to be evidenced and characterized in real atmospheric conditions.

In order to describe this multiphase chemistry and take gas/particle partitioning phenomena into account, a new analytical approach has recently been developed by Rossignol et al. (2012). It involves the simultaneous collection of both gaseous and particulate phases onto solid supports (adsorbent and filter), which are subsequently analyzed by thermal desorption coupled with gas chromatography and mass spectrometry (TD–GC/MS). Compared to previous works (Temime et al. 2007), this technique allows a rather easy detection of carbonyl compounds on the one side, and hydroxyl and carboxyl species, on the other side, using solid support derivatization procedures.

The present study, performed on a rural site of a Mediterranean island, Corsica, focused on the detection of limonene oxidation products by means of this new analytical method and relies for this purpose on a parent study performed in smog chamber experiment that involved the same new technique (Rossignol et al. 2012). A screening of other oxygenated species present in the field atmosphere was also performed in order to chemically characterize the collected organic matter as much as possible. One of the main objectives was to provide gas/particle partitioning coefficients of identified species under real conditions and compare them to theoretical values currently used in models to provide insight into the behavior of semi-volatile oxygenated compounds that are potentially influenced by still unaccounted specific processes.

1. Experimental

1.1. Sampling location and periods

The sampling site is a citrus field of around 30 ha belonging to the French National Institute for Agricultural Research (INRA). It is located in Corsica (France, Fig. S1) in a woody environment between Cervione and San Giuliano, small villages of 1600 and 600 inhabitants respectively, at 2 km from the eastern coast (9.5339744°E,42.2813633°N). The field is composed of a wide variety of citrus trees, including lemon, oranges, tangerine, citron, clementine, *etc*. It is surrounded by other tree species, like pine, implying the emission of wide range of biogenic VOC including limonene (Kesselmeier and Staudt 1999). This paper presents a snapshot of the atmospheric chemical composition as measured on June 23, 2011, as only two samples were taken during two consecutive periods, from 1 pm to 5 pm UTC and from 7 pm to 12 pm UTC. Nevertheless, these two samples were extremely useful to illustrate the analytical power of the protocol developed by Rossignol et al. (2012) and so, to provide an interesting insight on the physico-chemical behavior of oxidized organic atmospheric species. For these two sampling periods, low level (100 m) Hysplit back-trajectories (Draxler and Rolph 2014; Rolph 2014) provided with the Global Data Assimilation System (GDAS) meteorology fields from US National Weather Service at a resolution of 0.5° show that air masses were coming south-south-east, traveling in the boundary layer above Tyrrhenian Sea with no off-land contamination for more than 48 hr. Remarkably, the air masses that arrived on the sampling site from 1 pm to 5 pm had reached the Corsica coast from 30 min to 1.5 hr before, whereas the air masses that arrived on the sampling site from 7 pm to 12 pm had reached the coast from 2 to 5 hr before, possibly inducing differences in air masses chemical composition. Furthermore, higher level back-trajectories (500 m) show an even longer above-land transit for the evening air-masses. Globally, this indicates that both air masses sampled include a significant aged component with a very low fine aerosol loading while the second sample has probably been under a much stronger influence of in-land sources passing over fields and typical Mediterranean forest (with no major urbanized area).

1.2. Instrumentation for key parameters measurement

A weather station monitored temperature, relative humidity, wind speed and wind direction. Ozone concentration was measured by a 49i absorption ozone analyzer (49i, Thermo Electron Corporation, USA). $PM_{2.5}$ mass concentration was monitored with a Tapered Element Oscillating Microbalance (TEOM) (series 1400a, Rupprecht & Patashnick Co., USA) mounted with an Filter Dynamics Measurement System (FDMS) (series 8500, Rupprecht & Patashnick Co., USA). An optical particle counter (Grimm 1.108, Grimm Technologies, Germany) was used in parallel to estimate $PM_{2.5}$ and PM_1 mass concentrations, using a proportionality factor of 1 (taking into account the aerosol's density, refraction index and shape) to convert volume concentrations into mass concentrations. Limonene concentration was measured by an on-line gas

chromatograph equipped with a flame ionization detector and operated with an integration step of 15 min (airmo VOC GC 866, Chromatotec, France). The presence of other terpenes was checked by sampling air on 300 mg Tenax TA® sorbent tubes with subsequent off-line analysis by thermal-desorption coupled to gas chromatography and mass spectrometry (TD-GC/MS). A high volume sampler (DA80, Digitel, Switzerland) was used to collect $PM_{2.5}$ on quartz fiber filters for 24 hr (from 7 am on 23 June to 7 am on 24 June). On this 24 hr filter sample, thermo-optical measurements were performed (ECOC Lab Instrument model 5, Sunset Laboratory Inc., USA) to determine elemental and organic carbon mass fractions (EC/OC ratio, Cavalli et al. 2010). Organic matter (OM) loading was subsequently estimated from the OC value using an average OM/OC ratio of 2.3 similarly to Worton et al. (2011). Ion chromatography was used to quantify the major inorganic soluble species (nitrate, sulfate, ammonium, calcium, and sodium ions, Mihalopoulos et al. 1997). Sea salt loading was estimated as $2.54 \times [Na^+]$ (with $2.54 = (M_{Na} + M_{Cl}) / M_{Na}$, M being the molar mass of the element, and considering that sea salt contains only NaCl and that $[Na^+]$ is only of marine origin) and dust loading as $5.6 \times nss[Ca^{2+}]$ (with nss standing for "non sea salt" and $nss[Ca^{2+}] = [Ca^{2+}] - 0.038 \times [Na^+]$) (Guinot et al. 2007; Putaud et al. 2004).

1.3. Sampling and analysis of polar organic compounds

Gas and particulate phases were simultaneously and respectively collected on 300 mg Tenax TA® sorbent tubes (stainless steel ATD prepacked sample tubes, sorbent Tenax TA mesh 60/80, PerkinElmer Inc., USA) pre-coated with a derivatization reagent and 47 mm filters. Gas phase was collected at a flow rate of 50 mL/min downstream a Teflon filter (Zefluor, 47 mm, Pall Life Sciences, USA). Second pre-coated Tenax TA® tubes were placed downstream the first collection tubes to check for potential breakthrough of these latter. Particulate phase was collected on quartz and Teflon-quartz filters (QM-A grade, 47 mm, Whatman International Ltd., UK and Fiberfilm™, 47 mm, Pall Life Sciences, USA, respectively) using ChemComb cartridges (model 3500, Thermo Scientific, USA) equipped with $PM_{2.5}$ impactors and VOC denuders at a flow rate of $1 \, m^3/hr$. Field blanks of each sampling medium (non-exposed pre-coated sorbent tubes and filters) were set aside. All the field blanks and samples were derivatized and analyzed by thermal-desorption coupled to gas chromatography and mass spectrometry (TD–GC/MS). The entire sampling, derivatization and analysis method, specifically designed to quantify both the carbonyls and the hydroxyl and carboxylic compounds, have been reported in detail elsewhere (Rossignol et al. 2012). Briefly, for gas phase collection, the sorbent tubes were pre-coated before sampling either with o-(2,3,4,5,6-pentafluorobenzyl)hydroxylamine (PFBHA hydrochloride, puriss. p.a., derivatization grade for GC, 99.0%, Sigma Aldrich, Lyon, France) for the carbonyl compounds or with N-methyl-N-(t-butyldimethylsilyl)trifluoroacetamide containing 1% of tertbutyldimethylchlorosilane (MTBSTFA +1% t-BDMCS, Regis® Technologies Inc., Morton Grove, IL, USA) for the hydroxyl and carboxylic ones. In the case of hydroxyl bearing species and carboxylic acids, the sorbent tubes were re-exposed to MTBSTFA just before analysis, without any flow

and at a temperature of 60°C, to complete the derivatization process. Particles sampling were performed, on the one side, on quartz filters exposed just before analysis to PFBHA for the carbonyl compounds derivatization and, on the other, on Teflon-quartz filters exposed just before analysis to MTBSTFA for the hydroxyl and carboxylic compounds derivatization. The thermal desorption system was composed of (1) a multitubes auto-sampler (Ultra 50:50, Markes International, UK), (2) a platform desorber for single tubes (Unity 1, Markes International, UK) and (3) an air provider used in the mass flow controller mode (Air Server, Markes International, UK). Samples were desorbed at 300°C for 15 min at a flow rate of 50 mL/min and were cryogenically trapped on an adsorbent (Unity 1 cold trap, Tenax® TA, Markes International, UK) maintained at –10°C. The trap was desorbed for GC injection at 300°C, for 15 min with a split ratio of 1:9. GC/MS analysis were performed on a gas chromatograph (6890 A, Agilent Technologies, USA) equipped with an reversed-phase column (Rxi®-5Sil MS, 60 m, 0.25 mm i.d., film thickness 0.1 μm; Restek Corporation, USA) and coupled with a mass spectrometer (5973, Agilent Technologies, USA). Samples were chromatographically separated using a thermal ramp of 10°C/min from 40 to 305°C followed by a 10 min plateau, before returning to initial temperature. Quantification (or semi-quantification from a surrogate) was performed from the calibration curves presented in Rossignol et al. (2012). Compound concentrations were systematically corrected from field blanks.

To allow the identification of tracers from limonene oxidation and compare partitioning coefficients, these field results are compared to those of a parent study involving dark limonene ozonolysis in the European Photo-reactor (EuPhoRe) in Valencia, Spain, and the same gas and particulate phase analysis protocol of carbonyl and hydroxyl/carboxylic compounds (Rossignol et al. 2012). In this previous study, ca. 30 compounds were detected in the gas phase as PFBHA or MTBSTFA derivative products and ca. 65 in the particulate phase. All of these compounds were searched for in the present field campaign to assess whether limonene ozonolysis contributed to $PM_{2.5}$. A screening of other oxygenated species present in the field was also performed in order to better chemically characterize the atmospheric organic matter.

1.4. Calculation of experimental and theoretical partitioning coefficients

One of the originalities of this work lies in the simultaneous determination of gaseous and particulate phase concentrations of compounds, which makes it possible to provide on-site experimental (or measured) partitioning coefficients. For each compound i quantified in both gas and particulate phases, this experimental partitioning coefficient $K_{eff,i}$ ($m^3/\mu g$) was determined according to the following equation defined by Pankow (1994):

$$K_{eff,i} = \frac{A_p}{A_g M_o} \tag{1}$$

where, A_p and A_g ($\mu g/m^3$) are the concentration of the compound i in the organic particulate phase (of air) and in the gas

phase (of air), respectively, and M_o (µg/m³) is the concentration of the organic phase into which the compound is absorbed (of air). The equation assumes that the compound only condenses into the organic phase of particles. Uncertainties were calculated from calibration curve uncertainties for A_p and A_g (Rossignol et al. 2012) and from TEOM-FDMS measurement and OM uncertainties for M_o.

These experimental partitioning coefficients were compared to theoretical partitioning coefficients computed assuming equilibrium between the gas phase and an organic liquid phase, according to Pankow (1994):

$$K_{p,i} = \frac{760 \times 8202 \times 10^{-5} \times T}{M_{ow}\gamma_i \times 10^6 \times P_i^0} \tag{2}$$

where, P_i^0 (Torr) is the saturation vapor pressure, T (K) is the temperature, M_{ow} (g/mol) is the mean molar mass of the organic phase, and γ_i is the activity coefficient of the compound i in the organic phase. Activity coefficients were estimated with the universal functional group activity coefficient (UNIFAC) thermodynamic model (Fredenslund et al. 1975) based on the molecular structure of compounds identified in the organic phase.

The saturation vapor concentration C^* (µg/m³) was determined for all the tentatively identified compounds using the calculator of the extended aerosol inorganics model (Extended AIM) (Nannoolal et al., 2008, http://www.aim.env.uea.ac.uk/aim/aim.php).

2. Results and discussions

2.1. Key gas, particle and meteorological parameters

Fig. 1 shows the evolution of temperature, relative humidity, wind speed as well as the concentrations of ozone, limonene, PM$_{2.5}$ (Grimm and TEOM-FDMS measurements) and PM$_1$ (Grimm measurement only) on 23rd June, 2011 (UTC time). These diurnal profiles are similar to those observed on the same site, and with the same instrumentation, several days before and after this sampling day, as described thereafter.

The ozone concentration profile is quite typical, consistent with its photochemical formation cycle. It reached a maximum of about 75 µg/m³ at 9 am, remained steady during daytime, and started to decrease at about 6 pm to reach a concentration of about 20 µg/m³ at 10 pm. The limonene concentration also displayed strong diurnal variations, being close to zero during the day and increasing from 6 pm to reach a value of 7.5 µg/m³ around 8 pm. This is consistent with the study of Cahill et al. (2006) and Fares et al. (2012) in which higher monoterpene concentrations was observed at night than during the day. Here this nighttime increases can be explained by anincreased limonene lifetime as it was in the order of 3 hr at night (considering a ozone concentration of 20 ppbV and a null concentration in OH) and less than 15 min during daytime (considering a concentration of 70 ppbV in ozone and assuming a typical OH concentration of 5×10^6 radicals/cm³). It is also explained by a lower mixing height of the boundary layer concentrating the emitted monoterpenes. In the same way, PM$_{2.5}$ concentration also increases around
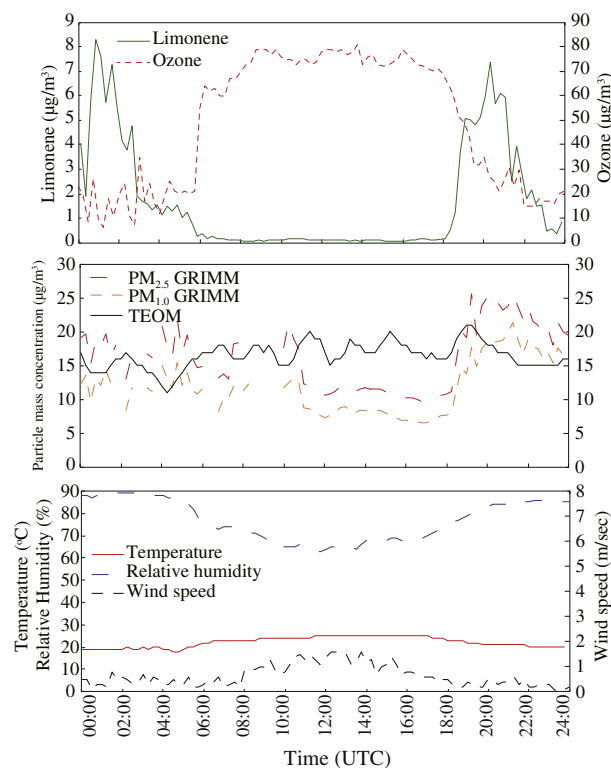

Fig. 1 – Variations of (a) limonene and ozone concentrations, (b) PM$_{2.5}$ (Grimm and TEOM measurements) and PM$_1$ concentration (Grimm measurement), and (c) temperature, relative humidity and wind speed on 23rd June, 2011. Grimm and TEOM refer to Section 1.2. TEOM: Tapered Element Oscillating Microbalance.

7 pm. OPC measurements show that this increase is driven by the finest fraction of the aerosol.

Besides limonene, other terpenes were detected by means of off-line gas phase sampling and GC–MS analysis without derivatisation: α- and β-pinene, Δ-carene, sabinene and γ-terpinene. Even if no quantification was performed, it was clear that the concentrations of these terpenes increased significantly in the evening compared to daytime, and displayed similar diurnal variations as the limonene one.

From 7 am on 23 June to 7 am on 24 June (according to 24 hr filter sampling), PM$_{2.5}$ mean concentrations were equal to 17 ± 4 µg/m³ according to TEOM-FDMS measurements. The mass composition of these PM$_{2.5}$ was determined as follows: 22% ± 4% of OM, 1.2% ± 0.2% of EC, 25% ± 2% of sulfate, 8% ± 1% of nitrate, 4% ± 1% of sea salt, 2.0% ± 0.4% of dust and 37% of unidentified matter. Even if photochemical conditions promote secondary species formation, the sulfate contribution was surprisingly high (25%) for a rural site, if one considers a mean contributions of 19% usually measured on European urban sites (Putaud et al. 2010). This could be explained by marine biogenic emissions, such as dimethyl-sulfide oxidation (Barnes et al. 2006), but could also suggest ananthropogenic influence such as urban pollution or more probably ship emissions (Corbett et al. 1999).

2.2. Polar organic compounds

Identification was proposed for 33 carbonyl compounds detected as PFBHA derivatives in the gaseous and particulate phases and for 26 hydroxyl/carboxylic compounds detected as MTBSTFA derivatives in the particulate phase. No data was obtained for gas phase hydroxyl/carboxylic compounds, which is probably due to the fact the relative humidity reached very high value at night overshooting the 70% RH value, which was the upper limit tested in Rossignol et al. (2012).

The lists of detected compounds were in good agreement between both sampling periods, afternoon and evening. In a same way, only small differences in quantification (within the uncertainty of the analytical protocol) were obtained, so that it appears irrelevant to propose any chemical consequence and/or explanation of the transition observed for ozone and limonene concentrations after 6 pm. If photo-chemical production of ozone stops in the evening explaining the drop, the limonene concentration raise seems mainly due to physical parameter changes, such as the decrease of the boundary layer height, without any direct consequence on the $PM_{2.5}$ composition. As a result, it is chosen to present thereafter only the detailed data obtained for the evening samples (Tables 1 and 2).

Overall, the sum of the quantified compounds in the particulate phase reached 430 ng/m^3, which corresponds to about 12% of the total mean organic matter concentration (3.7 ± 1.6 μg/m^3). The identified or tentatively identified compounds range from C_3 to C_{10} and bear up to three functionalities. Fifteen are shared with the EuPhoRe limonene ozonolysis study, suggesting a significant limonene oxidation contribution. Four of them are specific to this limonene oxidation: ketolimonene, limononaldehyde, ketonorlimonic acid and ketolimonic acid (Leungsakul et al. 2005; Jaoui et al. 2006). However, 3-carboxyheptanedioic acid, considered to be a tracer of aged limonene ozonolysis SOA (Jaoui et al. 2005) was not detected here, which is compatible with a freshly formed limonene SOA. For other compounds (methyl glyoxal, 4-oxopentanoic acid, hydroxybutanedioic acid), a multiple origin is likely, including the oxidation of other terpenes. Besides, pinene specific oxidation products were also detected, i.e., pinic acid, known for more than twenty years now to be formed from α- and β-pinene oxidation (Christoffersen et al. 1998), and 3-hydroxypentanedioic acid, identified by Claeys et al. (2007) as a marker for SOA from α-pinene oxidation.

2.2.1. Carbonyl species

Regarding the results for the carbonyl compounds, 2-butanone (17 ± 2 μg/m^3) and 2-hexanone (4.2 ± 0.4 μg/m^3) were the most abundant carbonyls in the gas phase. It was found later in the experimental field record that grass reaping was performed in the parcel around the sampling site during the sampling period. This high level of mechanical stress could have induce plant emission, which explain such an important concentration measured for 2-butanone (Isidorov et al. 1985; Kirstine et al. 1998; De Gouw et al. 1999; Kesselmeier and Staudt 1999; Bracho-Nunez et al. 2013). Nonanal (160 ± 20 ng/m^3), followed by glyoxal and methylglyoxal (40 ± 20 ng/m^3), were the most abundant carbonyls in the particulate phase. A wide range of linear monoaldehydes, including small ones (propanal to pentanal), could be observed in both phases. C_5 to C_{11}
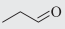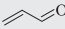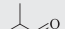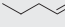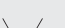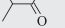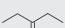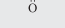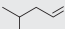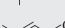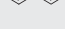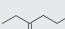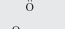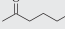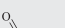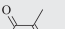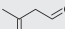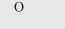
aldehydes have been considered to be of biogenic origin (Feng et al. 2005) and could be partially locally emitted. More precisely, it has been shown (Wildt et al. 2003) that these compounds are emitted by stressed species, e.g., when exposed to ozone or attacked by insects. Smaller aldehydes, propanal and butanal, can come from secondary (VOC oxidations) or primary sources (combustions) including ship fuel burning (Agrawal et al. 2008). Globally, n-aldehyde and n-carbonyl concentrations were similar to what has been previously reported in rural areas (Feng et al. 2005; Matsunaga et al. 2003) but much larger to what has been found in the boreal forest (Hellén et al. 2004) or in the Nashville (USA) area (McClenny et al. 1998).

The high concentrations measured for glyoxal and methylglyoxal, i.e., 40 ± 20 ng/m^3 in the particulate phase and 1.1 and 0.5 μg/m^3 respectively in gas phase, could suggest a significant anthropogenic influence on the air mass, even if both biogenic and anthropogenic VOC can lead to the formation of these two compounds. As an example of remote atmosphere, Kampf et al. (2012) measured in the Finnish boreal forest relatively low concentrations of glyoxal and methylglyoxal, 0.81 and 0.31 ng/m^3 respectively in the particulate phase. On the other side, concentrations above 10 ng/m^3 are often observed for urban aerosol samples (Kawamura and Yasui 2005). Even larger values have been found in rural area supposed to be exposed to long distance influence of polluted atmosphere (Kawamura et al. 2013 and reference therein). Together with the relatively high sulfate level observed in the aerosol samples, and in spite of the fact that no anthropogenic marker such as benzaldehyde or benzoic acid could be detected here, the measurement of such high concentrations of α-dicarbonyl species in both gas- and particulate phases can be related to the large scale antropization of the Mediterranean western basin.

The origin of 4-oxopentanal, detected in both gas and particulate phases, is likely multiple. As reported by Forester and Wells (2009), we detected it as a limonene oxidation product in chamber experiment (Rossignol et al. 2012). Limonene photooxidation and/or ozonolysis can thus be one of the sources of 4-oxopentanal. Heterogeneous oxidation of squalene and other terpenoids at the surface of the vegetation foliage can be another source of this compound, through the intermediate of 6-methyl-5-heptene-2-one (Fruekilde et al., 1998). In a forest atmosphere, Matsunaga et al. (2004) measured high concentrations of 4-oxopentanal, between 180 and 1570 ng/m^3 in the gas phase and between their detection limit (25 ng/m^3) and 207 ng/m^3 in the partic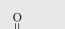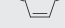ulate phase. The concentrations measured here (730 ± 30 ng/m^3 for the gas phase and 1.51 ± 0.06 ng/m^3 for the particulate phase) are consistent with these previous values. It is difficult here to propose a major origin of 4-oxopentanal (oxidation of terpenes vs. oxidation of squalene). The 6-methyl-5-heptene-2-one, an intermediate compound between squalene and 4-oxopentanal, was not detected in the present study, but it could be due to his short atmospheric life time compared with the 4-oxopentanal one (Fruekilde et al., 1998).

The quite ubiquitous isoprene oxidation products, methacrolein and methyl vinyl ketone, were not detected here. This must not be over interpreted as we have shown that on sorbent PFBHA derivation of methacrolein is of very low

Table 1 – Tentative/positive identification and quantification for detected carbonyl compounds, compared with rural and/or semi-rural literature data.

Compound	Structure	Identification	Quantification standard	Concentration (ng/m³)			
				This study		Other studies	
				Gas phase	Particulate phase	Gas phase	Particulate phase
Propanal		NIST EI lib.	Pentanal	1590 ± 50	13.2 ± 0.6	2000 [a] 50–850 [b]/80 [c]	
1-Propenal		From mass spectra	Pentanal	182 ± 6	4.1 ± 0.2		
Methylpropanal		From mass spectra	Pentanal	140 ± 5	1.15 ± 0.05		
2-Butanone		NIST EI lib.	2-Hexanone	17,000 ± 2000	nd	5200 [a]	
Butanal		NIST EI lib.	Pentanal	1920 ± 60	0.98 ± 0.04	1500 [a] 60–450 [b]/57 [c]	
3-Methyl-2-butanone		NIST EI lib.	2-Hexanone	nd	0.98 ± 0.02		
3-Pentanone		NIST EI lib.	2-Hexanone	1400 ± 200	nd		
3-Methylbutanal		NIST EI lib.	2-Ethylbutanal	60 ± 2	1.07 ± 0.01	340 [a]	
2-Butenal		NIST EI lib.	3-Methyl-2-butenal	132 ± 2	1.75 ± 0.09	150 [a]	
Pentanal		NIST EI lib.	Pentanal	820 ± 30	0.56 ± 0.03	630 [a]/7–120 [b] 46 [c]	
3-Hexanone		NIST EI lib.	2-Hexanone	540 ± 5	nd		
2-Hexanone		NIST EI lib.	2-Hexanone	4200 ± 400	nd		
3-Heptanone		NIST EI lib.	4-Heptanone	660 ± 30	nd		
Hexanal		NIST EI lib.	Pentanal	440 ± 20	nd	550 [a]/40–330 [b] 48 [c]	
2-Heptanone		NIST EI lib.	4-Heptanone	650 ± 30	nd		
3-Octanone		From mass spectra	4-Heptanone	600 ± 30	nd		
Cyclohexanone		NIST EI lib.	Carvone	680 ± 70	nd		
Heptanal	$nC_7H_{14}O$	NIST EI lib.	Heptanal	268 ± 5	nd	300 [a]	
Octanal	$nC_8H_{16}O$	NIST EI lib.	Heptanal	411 ± 7	30 ± 3	350 [a] 82 [c]	
Nonanal	$nC_9H_{18}O$	NIST EI lib.	Heptanal	790 ± 20	160 ± 20	1700 [a] 3–241 [d]	0–262 [d]
Ketolimonene		From mass spectra	Dihydrocarvone	**135 ± 3**	**nd**		
Decanal	$nC_{10}H_{20}O$	NIST EI lib.	Heptanal	750 ± 20	nq	440 [a]/88 [c] 16–249 [d]	1–1.6 [e] 16–290 [d]
Glyoxal		Standard	Glyoxal	1100 ± 200	40 ± 20	50–1450 [b]	8.3–11 [e]
Methylglyoxal		Standard	Methylglyoxal	**500 ± 200**	**40 ± 20**	150–6000 [b]	26–33 [e]
Dimethyglyoxal		Standard	Dimethylglyoxal	**1800 ± 200**	**3.7 ± 0.6**		
3-Oxobutanal or Butanedial		From mass spectra	4-Oxopentanal	nq (coel.)	nq		
4-Oxopentanal		Standard	4-Oxopentanal	**730 ± 30**	**1.51 ± 0.06**	180–1570 [f]	0–207 [f]
2,5-Hexanedione		From mass spectra	3-Methyl-2,4-pentanedione	470 ± 30	nd		
1,3 or 1,2 Dioxocyclopentene		From mass spectra	4-Oxopentanal	53 ± 2	1.06 ± 0.05		
4-Oxo-2-pentenal		From mass spectra	4-Oxopentanal	nd	0.51 ± 0.02		
Limononaldehyde		From mass spectra	4-Oxopentanal	**245 ± 8**	**nd**		
2-Isopropenebut-2-enedial		From mass spectra	4-Oxopentanal	nd	0.88 ± 0.04		

efficiency (Rossignol et al. 2012). Given the similarity of the two structures, low efficiency derivatization is also expected for methyl vinyl ketone.

2.2.2. Hydroxyl and carboxylic species

Mono carboxylic acids, pentanoic acid (38 ± 2 ng/m^3), hexanoic acid (26 ± 1 ng/m^3), heptanoic acid (13 ± 2 ng/m^3) and nonanoic acids (17 ± 3 ng/m^3) were the most abundant hydroxyl and carboxylic acid compounds in the particulate phase. Their origin is uncertain as they can be either of primary or secondary, coming from biogenic or anthropogenic precursors and being formed in the atmosphere from hydrocarbons gas-phase oxidations and carbonyl aqueous-phase oxidations (Chebbi and Carlier 1996). Other long chain carboxylic acids (dodecanoic, tridecanoic, octadecanoic acid, hexadecanoic, etc.) were also measured. They are expected to be from primary biogenic or anthropogenic origin (Fang et al. 2002). Their concentrations, below 20 ng/m^3, were lower than concentrations measured by Cahill et al. (2006) in the Sierra Nevada mountains of California, especially for hexadecanoic acid, which was about ten times lower in our study. They were nevertheless similar to those measured by Limbeck et al. (2001) on a rural site in South Africa.

C_4 to C_6 saturated dicarboxylic acids were also detected and quantified. Possible origins include oxidation of oleic acid (Legrand et al. 2007) and ozonolysis of cyclohexene coming from both biogenic and anthropogenic sources (Hamilton et al. 2006). These diacids were also detected in our simulation chamber limonene ozonolysis experiment (Rossignol et al. 2012), suggesting the possibility of an additional biogenic precursor oxidation origin. Among these diacids, but anedioic acid was the most abundant with a concentration of 10 ± 4 ng/m^3 in the particulate phase. This concentration was quite similar to those measured by Limbeck et al. (2001). More generally speaking, the measured concentrations of dicarboxylic acids are comparable to levels measured on a rural site by Röhrl and Lammel (2002).

Detected hydroxydicarboxylic acids, hydroxybutanedioic acid, 2- and 3-hydroxypentanedioic acids and 3-hydroxyhexanedioic acid, are likely to arise from the oxidation of biogenic precursors. They were indeed detected in the limonene ozonolysis experiment (Rossignol et al. 2012), while Jaoui et al. (2008) identified 3-hydroxypentanedioic acid as an oxidation product of pinene and Claeys et al. (2007) described it as a good tracer for α-pinene oxidation.

2.2.3. Oxidation state of particulate phase compounds

All the compounds detected in both gas and particulate phases have been reported on a 2D framework (Fig. 2) adapted from Jimenez et al. (2009). This framework presents the oxidation state, represented by the compound atomic O:C ratio, as a function of volatility, represented by the logarithm of the saturation vapor concentration of the given compound C^* (μg/m^3). C^* is defined as $1/K$, where, K (m^3/μg) is the partitioning coefficient of the compound (Donahue et al. 2006) and is determined here from the compound saturation vapor pressure, calculated using the method reported by Nannoolal et al. (2008). Three groups of compounds seem to stand out, tentatively define on the graph by the areas I, II and III. Group I refers mainly to mono- and di-carbonyl species with a relatively low oxidation state and theoretical log C^* being between 5 and 9. This range of volatility corresponds to highly volatile species expected to significantly partition into the particulate phase only at very high particulate OM concentration (Donahue et al. 2009). Nevertheless, while the OM concentration was only of about 3.7 μg/m^3, most of the small aldehydes, including propanal, propenal and butyraldehyde that could come from ship emissions (Agrawal et al. 2008), i.e., long range transport, were detected into the particulate phase. On the contrary, most of the ketones, including 2-butanone, ketolimonene and limononaldehyde expected to be locally emitted, were only detected in the gas phase. This could suggest that along with the intrinsic volatility of the compound, the age of the compound into the air mass might be of importance regarding its partitioning behavior. Group II refers to bi-functionalized species and group III to tri-functionalized ones bearing at least one carboxylic acid group. No data was obtained in this study on the gas phase concentration of these species, but the compounds in these two groups are highly oxidized and, as expected, partition into the particulate phase. Some of these poly-functionalized species, such as ketolimonic acid, ketonorlimonic acid, pentanedioic acid or 3-hydroxyhexanedioic acid, are likely second generation oxidation products. Fig. 2 strongly suggests that the aerosol population on the sampling site is resulted from a mixture between primary emitted compounds, freshly formed pinene and limonene SOA and more processed organic matter, e.g., transported over long distance.

2.3. Comparison of experimentaland theoretical partitioning coefficients

As the technique deployed in this work has allowed, for some of the carbonyls, the determination of the concentration in both gaseous and particulate phase, it is an opportunity to calculate related partitioning coefficients. These datasets measured under various real conditions are still rather rare,

Notes to Table 1:
NIST EI lib.: Electron Impact mass spectra library of the National Institute of Standard and Technology of the U.S. department of commerce; nd: not detected; nq: not quantified (hindered by co-elutions); in bold: compounds detected both in this study and in the parent smog chamber experiment (Rossignol et al. 2012).
[a] (Feng et al., 2005).
[b] (Cerqueira et al., 2003).
[c] Hellén et al., 2004.
[d] (Matsunaga et al., 2003).
[e] (Cahill et al., 2006).
[f] (Matsunaga et al., 2004).

Table 2 – Tentative/positive identification and quantification for observed hydroxyl compounds and carboxylic acids.

Compound	Structure	Identification	Quantification standard	Particulate phase concentration (ng/m³)	
				This study	Other studies
Pentanoic acid		Standard	Pentanoic acid	38 ± 2	
Hexanoic acid		From mass spectra	Pentanoic acid	25.6 ± 0.9	
4-Oxopentanoic acid		Standard	4-Oxopentanoicacid	**6 ± 3**	
Heptanoic acid		Standard	Heptanoic acid	13 ± 2	
Hydroxyacetic acid		NIST EI lib.	No relevant standard available	nq	
2-Hydroxy-2-methylpropanoic acid		NIST EI lib.	No relevant standard available	nq	
3-Hydroxypropanoic acid		NIST EI lib.	No relevant standard available	nq	
Nonanoic acid	nC$_9$H$_{18}$O$_2$	NIST EI lib.	Heptanoic acid	17 ± 3	
Butanedioic acid		NIST EI lib.	Butanedioic acid	**10 ± 4**	1.9–12.4 [a]/5.5 [b] 4.8–31.1 [c]/9.42–12.0 [d]
2-Methylbutanedioic acid		Standard	Butanedioic acid	**0.9 ± 0.4**	1.12–1.56 [d]
Trans-butenedioic acid		NIST EI lib.	Butanedioic acid	1.8 ± 0.7	0.4 [c]/14.3 [e]
Pentanedioic acid		NIST EI lib.	Butanedioic acid	**0.7 ± 0.3**	5.8 [b]/0.7–4.0 [c] 1.96–3.50 [d]/1.2 [e]
Dodecanoic acid	nC$_{12}$H$_{24}$O$_2$	NIST EI lib.	Heptanoic acid	1.5 ± 0.2	9.8 [b] 0.3–0.8 [c]
2,3-Dihydroxypropanoic acid		NIST EI lib.	No relevant standard available	nq	1.3–5.5 [f]
Hexanedioic acid		NIST EI lib.	Butanedioic acid	**0.21 ± 0.09**	2.2–9.5 [a]/0.6–15.9 [c] 1.06–1.89 [d]
Tridecanoic acid	nC$_{13}$H$_{26}$O$_2$	NIST EI lib.	Heptanoic acid	0.44 ± 0.06	1.7 [b]
Ketonorlimonic acid		From mass spectra	No relevant standard available	**0.20** [*]	
Hydroxybutanedioic acid		Standard	Hydroxybutanedioicacid	**2.4 ± 0.6**	22-62 [a]/2.2 [b] 11.2 [e]/3-26 [f]
Pinic acid		Standard	Pinic acid	0.41 ± 0.07	0.4-135 [a]/4.3 [b] 1-10 [f]/0.35–1.19 [g]
Ketolimonic acid		From mass spectra	No relevant standard available	**0.15** [*]	
3-Hydroxypentanedioic acid		From mass spectra	Hydroxybutanedioic acid	0.8 ± 0.2	1.5-113 [a] 1.6-14 [f]
2-Hydroxypentanedioic acid		NIST EI lib.	Hydroxybutanedioic acid	**0.7 ± 0.2**	0.6–3.6 [a]
Hexadecanoic acid	nC$_{16}$H$_{32}$O$_2$	NIST EI lib.	Heptanoicacid	8 ± 1	39-140 [b]
3-Hydroxyhexanedioic acid		From mass spectra	Hydroxybutanedioic acid	**0.31 ± 0.08**	
Octadecanoic acid	nC$_{18}$H$_{36}$O$_2$	NIST EI lib.	Heptanoic acid	1.4 ± 0.2	12-31 [b] 0.13–1.67 [d]

In bold: compounds detected both in this study and in the parent smog chamber experiment (Rossignol et al. 2012).

[a] Kourtchev et al. 2008 and references therein.
[b] Cahill et al. 2006.
[c] Limbeck et al. 2001.
[d] Zheng et al. 2002.
[e] Kuo et al. 2011.
[f] Fu and Kawamura 2011.
[g] Gómez-González et al., 2012).
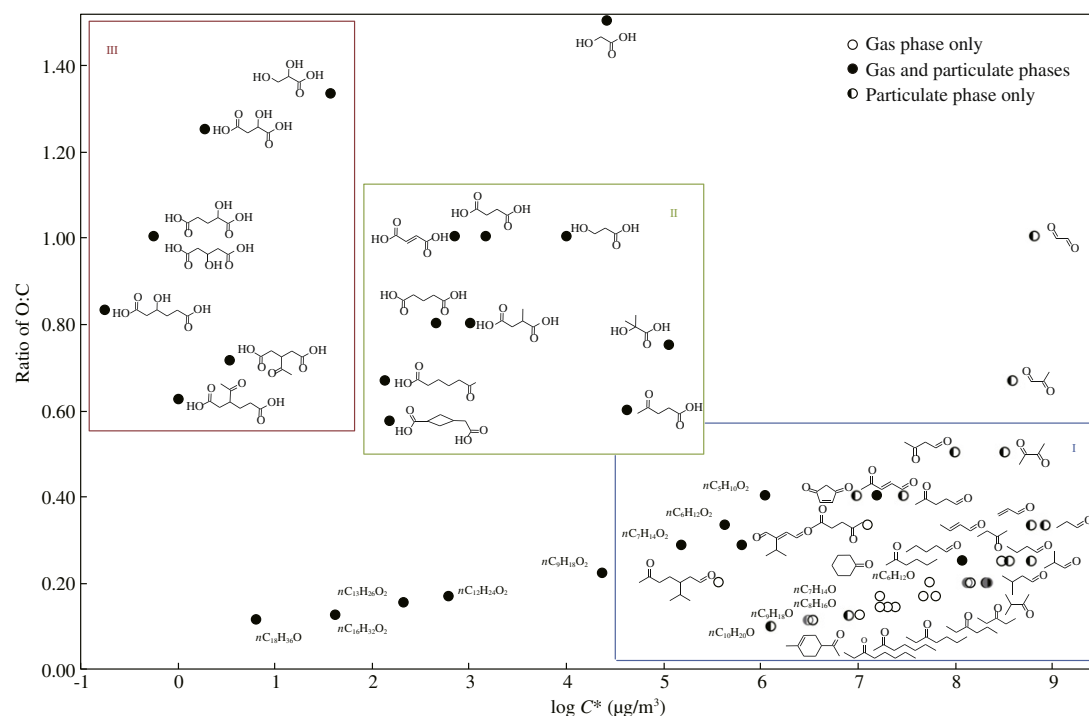[*] Estimation based on a pinic acid calibration curve.

Fig. 2 – 2D framework representing oxidation state (approximated by ratio of O:C) vs. volatility ($\log_{10}C^*$ at 295 K) for all the organic species detected on 23rd June, 2011. Adapted from Jimenez et al. (2009). C^* is defined as $1/K$, where, K is the partitioning coefficient of the compound; group I refers to mono- and di-carbonyl species, group II refers to bi-functionalized species and group III to tri-functionalized ones.

in spite of the fact that they are required to assess the relevance of the partitioning parameterization and improve SOA modeling based either on theoretical vapor pressure estimation using group contribution methods (Valorso et al. 2011) or on data fitting from experimental studies (Couvidat et al. 2012).

Here, experimental partitioning coefficients were determined from the gas and particulate phases compound concentrations presented in Table 1 and a value for the organic matter loading (OM, equivalent to M_o in Eq. (1)) of the aerosol population estimated at 3.7 ± 1.6 μg/m³ from OC measurement (see Section 2.1). The resulting data set is presented in Table 3, where it is compared to experimental partitioning coefficients measured by Rossignol et al. (2012) in the EuPhoRe smog chamber for limonene ozonolysis experiments and to theoretical partitioning coefficients. These theoretical coefficients were computed assuming equilibrium between the gas phase and an organic liquid phase and following Eq. (2). The saturation vapor pressure of each compound was evaluated at 293 and 298 K (respectively the minimum and the maximum temperatures, T_{min} and T_{max}, observed during the sampling period). Data used for this computation can be found in Appendix A. Supplementary data.

A total of 12 cases were considered for activity coefficient γ_i estimation, covering a relevant range of partitioning conditions:

(1) Two cases for temperature, *i.e.*, 293 and 298 K, respectively T_{min} and T_{max} of the sampling period;

(2) Three cases for taking into account relative humidity conditions, *i.e.*, with and without water partitioning in the organic phase (quantity of water estimated thanks to the Raoult's law from the relative humidity) and with 2 different relative humidities in the case of water partitioning, RH_{min} 50% (at T_{min}) and RH_{max} 80% (at T_{max});

(3) Three cases concerning the nature of the unidentified organic mass: (i) Unidentified organic mass was not taken into account; (ii) It was considered to be highly oxidized and one of the most oxygenated detected compound, 3-hydroxyhexandioic acid, was used as a molecular structure to mimic the unidentified fraction; (iii) It was considered to be poorly oxidized and one of the less polar detected compound, decanal, was used as a molecular structure to mimic the unidentified fraction. The resulting γ_i values (minimum, maximum and mean values) are provided in Appendix A. Supplementary data. The corresponding partitioning coefficients values (minimum, maximum and mean values), also taking into account T_{min} and T_{max} values for saturation vapor pressure estimation, are presented in Table 3.

Whatever the conditions applied for computation, the theoretical partitioning coefficients $K_{p,i}$ are always several orders of magnitude smaller than the experimentally measured ones. In other words, the semi-volatile species for which this comparison was performed seem to partition more into the particulate phase, *i.e.*, contribute more to the SOA mass, than expected. The hypothesis of a positive artifact on

Table 3 – Citrus field experimental partitioning coefficients ($K_{eff,i}$) compared with smog chamber experimental $K_{eff,i}$ determined in Rossignol et al. (2012) and estimated $K_{p,i}$ (units: m^3/μg).

Compound	Citrus field $K_{eff,i}$	EuPhoRe $K_{eff,i}$	Mean estimated $K_{p,i}$	Min estimated $K_{p,i}$	Max estimated $K_{p,i}$
Propanal	$2.2 \times 10^{-3} \pm 50\%$		3.3×10^{-10}	6.0×10^{-11}	5.4×10^{-10}
1-Propenal	$6.1 \times 10^{-3} \pm 50\%$		2.1×10^{-10}	3.2×10^{-11}	4.6×10^{-10}
Methylpropanal	$2.2 \times 10^{-3} \pm 50\%$		5.1×10^{-10}	7.0×10^{-11}	8.9×10^{-10}
Butanal	$1.4 \times 10^{-4} \pm 49\%$		8.0×10^{-10}	1.1×10^{-10}	1.4×10^{-9}
3-Methylbutanal	$4.8 \times 10^{-3} \pm 46\%$		1.0×10^{-9}	1.1×10^{-10}	1.7×10^{-9}
2-Butenal	$3.6 \times 10^{-3} \pm 49\%$		1.7×10^{-9}	2.0×10^{-10}	3.8×10^{-9}
Pentanal	$1.8 \times 10^{-4} \pm 51\%$		2.3×10^{-9}	2.2×10^{-10}	4.7×10^{-9}
Octanal	$2.0 \times 10^{-2} \pm 54\%$		3.0×10^{-8}	1.0×10^{-9}	7.2×10^{-8}
Nonanal	$5.5 \times 10^{-2} \pm 57\%$		7.0×10^{-8}	1.68×10^{-9}	2.2×10^{-7}
Glyoxal	$9.8 \times 10^{-3} \pm 110\%$		5.7×10^{-11}	2.3×10^{-12}	2.6×10^{-10}
Methylglyoxal	$2.2 \times 10^{-2} \pm 132\%$	$1.3 \times 10^{-3} \pm 84\%$	2.6×10^{-10}	8.4×10^{-12}	1.6×10^{-9}
Dimethylglyoxal	$5.6 \times 10^{-4} \pm 70\%$	$6.2 \times 10^{-4} \pm 47\%$	6.4×10^{-10}	4.15×10^{-11}	2.6×10^{-9}
4-Oxopentanal	$5.6 \times 10^{-4} \pm 50\%$	$6.5 \times 10^{-4} \pm 34\%$	3.0×10^{-8}	9.7×10^{-10}	1.6×10^{-7}
Dioxocyclopentene	$5.4 \times 10^{-3} \pm 51\%$		5.4×10^{-8}	1.2×10^{-9}	3.7×10^{-7}

the particulate phase measurements explaining alone the observed discrepancies can be reasonably excluded as VOC denuders were used upstream the filters. Moreover, similar discrepancies between experimental and theoretical values were previously evidenced in the few studies having had the same objective of determining experimental coefficients. Matsunaga et al. (2005); Healy et al. (2008) and Kawamura et al. (2013) also measured experimental partitioning coefficients several orders of magnitude larger than those predicted by the theory, using comparable derivatization techniques. More recently, new works based on on-line mass spectrometry measurements analysis of both phases without any derivatization pretreatment, have led to similar conclusions (Gensch et al. 2013; Steitz et al. 2013).

One explanation could be that the instantaneous equilibrium between the gas phase and the organic liquid phase, assumed by theoretical calculations, is not achieved. There are indeed some recent evidences that the aerosol organic phase can be highly viscous and act like a semi-solid phase (Virtanen et al. 2010; Shiraiwa et al. 2011). In such a case, the compounds cannot reach the partitioning equilibrium instantaneously. Esterification for instance, as demonstrated by Zhang et al. (2011) when studying of the fate of methylglyceric from isoprene oxidation, can participate in oligomers formation and therefore increase SOA viscosity. This can become significant for volatile compounds that were measured here as being surprisingly abundant in the particulate phase. Since those compounds are volatile, they should not be present in large amount in the particle phase, unless intra-particulate reactions are involved. Under favorable conditions, i.e., at low aerosol water content, carbonyl compounds can undergo oligomerization reactions, such as acetalisation. Indeed, Jang et al. (2003) observed aerosol growth by heterogeneous hemiacetal/acetal acid-catalyzed reaction of carbonyl compounds on particle surfaces. They demonstrated that aldehydes are more reactive than ketone. Liggio et al. (2005) shed light on the glyoxal self-reaction to form cyclic acetal. They also showed that these oligomerization reactions are not favored at high humidity and can potentially release the monomeric volatile compounds into the particulate phase under such conditions. At high humidity, the formed oligomers would thus give back the monomers, which could reach the concentrations measured here if the

organic phase is viscous. Indeed, Grieshop et al. (2007) have shown from chamber experiments that semi-volatils from SOA take hours to repartition after dilution of the reacting mixture showing that the partition can remain off-equilibrium for hours.

This non-equilibrium hypothesis between the gas and the particulate phases is only acceptable for aged aerosol components. On the contrary, it can be assumed that limononaldehyde is a quite locally formed compound, as it is directly produced by limonene photooxidation and/or ozonolysis. Here, the measured limononaldehyde gas phase concentration was significant, 245 ± 8 ng/m^3, whereas its particulate phase concentration was below the detection limit of the analytical method (0.008 ng/m^3 for a 5 m^3 sampling volume, Rossignol et al. 2012). Its experimental partitioning coefficient is consequently assumed to be equal to or lower than 8.8×10^{-6} m^3/μg. Whatever the case, this limononaldehyde experimental partitioning coefficient is lower than those measured here for expected more volatile carbonyl compounds and is quite close to the theoretical ones estimated for this compound at 298 K, ranging from 1.4×10^{-6} to 7.5×10^{-6} m^3/μg (Rossignol et al. 2012). This can be considered as an additional clue indicating that the gas/particle partitioning behavior a compound can be strongly related to the age of this compound in the air mass and to the air mass history, this latter influencing both particulate phase reactivity and mass transfers, limited by aerosol viscosity.

3. Conclusions and perspectives

This work provides a comprehensive chemical characterization of polar organic compounds in gas and particulate phases sampled on a rural Mediterranean site in northern Corsica on 23 June, 2011. Experimental partitioning coefficients of carbonyl compounds were inferred from these measurements. These data were completed with back-trajectory calculation and the measurement of more global parameters such as gas phase limonene, ozone or PM$_{2.5}$ concentrations as well as organic carbon, elementary carbon and inorganic contents of PM$_{2.5}$. About sixty carbonyl, hydroxyl and carboxylic acids,

ranging from C_3 to C_{18} and from mono to trifunctionalised compounds, were positively or tentatively identified in gas and/or particulate phases. Back-trajectories together with the measurement of relatively high concentration of sulfates and α-dicarbonyls suggest a long distance influence of anthropogenic contamination such as ship emissions. Besides, detection of n-aldehydes, hydroxydicarboxylic acids and limonene and pinene oxidation products shows a quite rational biogenic influence on the air mass. Comparison of on-site experimental partitioning coefficients determined for a series of carbonyl compounds with theoretical ones reveals discrepancies of several orders of magnitudes, most of carbonyls portioning much more into the particulate phase than expected, in agreement with previous studies. This is specifically true for the compounds having potentially long range transport origin. On the contrary, an expected locally emitted compound, limononaldehyde, displayed an experimental partitioning coefficient much closer to theoretical calculation, i.e., partitioned as expected or less into the particulate phase. These observations are additional clues suggesting that an instantaneous equilibrium assumption between the gas and an organic liquid phase is not valid when aged aerosol is involved, and that, maybe, aerosol viscosity should be taken into account together with air mass age and history in order to better assess individual gas/particle partitioning behaviors.

This work is a step further in the comprehension of the complex multiphase processes involved in real atmospheres. Besides a detailed speciation of the oxygenated fraction of the atmospheric organic matter, it underlines the importance of taking volatile species into account in SOA related processes assessment as well as the possible influence of viscosity, air mass age and history on the partitioning behavior of these compounds.

Acknowledgment

Appendix A. Supplementary data

Supplementary data to this article can be found online at http://dx.doi.org/10.1016/j.jes.2015.11.017.

REFERENCES

Agrawal, H., Welch, W.A., Miller, J.W., Cocker, D.R., 2008. Emission measurements from a crude oil tanker at sea. Environ. Sci. Technol. 42 (19), 7098–7103.

Asher, W.E., Pankow, J.F., 2006. Vapor pressure prediction for alkenoic and aromatic organic compounds by a UNIFAC-based group contribution method. Atmos. Environ. 40 (19), 3588–3600.

Barnes, I., Hjorth, J., Mihalopoulos, N., 2006. Dimethyl sulfide and dimethyl sulfoxide and their oxidation in the atmosphere. Chem. Rev. 106 (3), 940–975.

Bracho-Nunez, A., Knothe, N.M., Welter, S., Staudt, M., Costa, W.R., Liberato, M.A.R., et al., 2013. Leaf level emissions of volatile organic compounds (VOC) from some Amazonian and Mediterranean plants. Biogeosciences 10 (9), 5855–5873.

Cahill, T.M., Seaman, V.Y., Charles, M.J., Holzinger, R., Goldtsein, A.H., 2006. Secondary organic aerosols formed from oxidation of biogenic volatile organic compounds in the Sierra Nevada Mountains of California. J. Geophys. Res. 111 (D16), D16312.

Cavalli, F., Viana, M., Yttri, K.E., Genberg, J., Putaud, J.P., 2010. Toward a standardised thermal-optical protocol for measuring atmospheric organic and elemental carbon: the EUSAAR protocol. Atmos. Meas. Tech. 3 (1), 79–89.

Cerqueira, M.A., Pio, C.A., Gomes, P.A., Matos, J.S., Nunes, T.V., 2003. Volatile organic compounds in rural atmospheres of central Portugal. Sci. Total Environ. 313 (1–3), 49–60.

Chebbi, A., Carlier, P., 1996. Carboxylic acids in the troposphere, occurrence, sources and sinks: a review. Atmos. Environ. 30 (24), 4233–4249.

Christoffersen, T.S., Hjorth, J., Horie, O., Jensen, N.R., Kotzias, D., Molander, L.L., et al., 1998. Cis-Pinic acid, a possible precursor for organic aerosol formation from ozonolysis of α-pinene. Atmos. Environ. 32 (10), 1657–1661.

Claeys, M., Szmigielski, R., Kourtchev, I., Van der Veken, P., Vermeylen, R., Maenhaut, W., et al., 2007. Hydroxydicarboxylic acids: markers for secondary organic aerosol from the photooxidation of α-pinene. Environ. Sci. Technol. 41 (5), 1628–1634.

Corbett, J.J., Fischbeck, P.S., Pandis, S.N., 1999. Global nitrogen and sulfur inventories for oceangoing ships. J. Geophys. Res. Atmos. 104 (D3), 3457–3470.

Couvidat, F., Debry, É., Sartelet, K., Seigneur, C., 2012. A hydrophilic/hydrophobic organic (H^2O) aerosol model: development, evaluation and sensitivity analysis. J. Geophys. Res. Atmos. 117 (D10), D10304.

De Gouw, J.A., Howard, C.J., Custer, T.G., Fall, R., 1999. Emissions of volatile organic compounds from cut grass and clover are enhanced during the drying process. Geophys. Res. Lett. 26 (7), 811–814.

Donahue, N.M., Robinson, A.L., Stanier, C.O., Pandis, S.N., 2006. Coupled partitioning, dilution, and chemical aging of semivolatile organics. Environ. Sci. Technol. 40 (8), 2635–2643.

Donahue, N.M., Robinson, A.L., Pandis, S.N., 2009. Atmospheric particulate matter: from smoke to secondary organic aerosol. Atmos. Environ. 43 (1), 94–106.

Draxler, R.R., Rolph, G.D., 2014. HYSPLIT-Hybrid single particle lagrangian integrated trajectory model. (Available at: http://www.arl.noaa.gov/HYSPLIT.php. Date accessed: 11 June 2015).

Fang, J.S., Kawamura, K., Ishimura, Y., Matsumoto, K., 2002. Carbon isotopic composition of fatty acids in the marine aerosols from the Western North Pacific: implication for the source and atmospheric transport. Environ. Sci. Technol. 36 (12), 2598–2604.

Fares, S., Park, J.H., Gentner, D.R., Weber, R., Ormeño, E., Karlik, J., et al., 2012. Seasonal cycles of biogenic volatile organic compound fluxes and concentrations in a California citrus orchard. Atmos. Chem. Phys. 12 (20), 9865–9880.

Feng, Y.L., Wen, S., Chen, Y.J., Wang, X.M., Lü, H.X., Bi, X.H., et al., 2005. Ambient levels of carbonyl compounds and their sources in Guangzhou, China. Atmos. Environ. 39 (10), 1789–1800.

Forester, C.D., Wells, J.R., 2009. Yields of carbonyl products from gas-phase reactions of fragrance compounds with OH radical and ozone. Environ. Sci. Technol. 43 (10), 3561–3568.

Fredenslund, A., Jones, R.L., Prausnitz, J.M., 1975. Group-contribution estimation of activity coefficients in nonideal liquid mixtures. AICHE J. 21 (6), 1086–1099.

Fruekilde, P., Hjorth, J., Jensen, N.R., Kotzias, D., Larsen, B., 1998. Ozonolysis at vegetation surfaces: a source of acetone, 4-oxopentanal, 6-methyl-5-hepten-2-one, and geranyl acetone in the troposphere. Atmos. Environ. 32 (11), 1893–1902.

Fu, P.Q., Kawamura, K., 2011. Diurnal variations of polar organic tracers in summer forest aerosols: a case study of a *Quercus* and *Picea* mixed forest in Hokkaido, Japan. Geochem. J. 45 (4), 297–308.

Gensch, I., Hohaus, T., Kimmel, J., Jayne, J.T., Worsnop, D.R., Kiendler-Scharr, A., 2013. Experimental Determination of Partition Coefficient for Beta-Pinene Ozonolysis Products in SOA. EGU General Assembly, Vienna, Austria.

George, I.J., Abbatt, J.P.D., 2010. Heterogeneous oxidation of atmospheric aerosol particles by gas-phase radicals. Nature Chem. 2 (9), 713–722.

Gómez-González, Y., Wang, W., Vermeylen, R., Chi, X., Neirynck, J., Janssens, I.A., et al., 2012. Chemical characterisation of atmospheric aerosols during a 2007 summer field campaign at Brasschaat, Belgium: sources and source processes of biogenic secondary organic aerosol. Atmos. Chem. Phys. 12 (1), 125–138.

Graber, E.R., Rudich, Y., 2006. Atmospheric HULIS: how humic-like are they? A comprehensive and critical review. Atmos. Chem. Phys. 6 (3), 729–753.

Grieshop, A.P., Donahue, N.M., Robinson, A.L., 2007. Is the gas–particle partitioning in α-pinene secondary organic aerosol reversible? Geophys. Res. Lett. 34 (14), L14810.

Guinot, B., Cachier, H., Oikonomou, K., 2007. Geochemical perspectives from a new aerosol chemical mass closure. Atmos. Chem. Phys. 7 (6), 1657–1670.

Hallquist, M., Wenger, J.C., Baltensperger, U., Rudich, Y., Simpson, D., Claeys, M., et al., 2009. The formation, properties and impact of secondary organic aerosol: current and emerging issues. Atmos. Chem. Phys. 9 (14), 5155–5236.

Hamilton, J.F., Lewis, A.C., Reynolds, J.C., Carpenter, L.J., Lubben, A., 2006. Investigating the composition of organic aerosol resulting from cyclohexene ozonolysis: low molecular weight and heterogeneous reaction products. Atmos. Chem. Phys. 6 (12), 4973–4984.

Healy, R.M., Wenger, J.C., Metzger, A., Duplissy, J., Kalberer, M., Dommen, J., 2008. Gas/particle partitioning of carbonyls in the photooxidation of isoprene and 1,3,5-trimethylbenzene. Atmos. Chem. Phys. 8 (12), 3215–3230.

Hellén, H., Hakola, H., Reissell, A., Ruuskanen, T.M., 2004. Carbonyl compounds in boreal coniferous forest air in Hyytiälä, Southern Finland. Atmos. Chem. Phys. 4 (7), 1771–1780.

IPCC, 2007. Fourth Assessment Report: Climate Change 2007: The Physical Science Basis. Cambridge University Press, Cambridge, United Kingdom and New York, NY, USA.

Isidorov, V.A., Zenkevich, I.G., Ioffe, B.V., 1985. Volatile organic compounds in the atmosphere of forests. Atmos. Environ. 19 (1), 1–8.

Jang, M., Carroll, B., Chandramouli, B., Kamens, R.M., 2003. Particle growth by acid-catalyzed heterogeneous reactions of organic carbonyls on preexisting aerosols. Environ. Sci. Technol. 37 (17), 3828–3837.

Jaoui, M., Kleindienst, T.E., Lewandowski, M., Offenberg, J.H., Edney, E.O., 2005. Identification and quantification of aerosol polar oxygenated compounds bearing carboxylic or hydroxyl groups. 2. Organic tracer compounds from monoterpenes. Environ. Sci. Technol. 39 (15), 5661–5673.

Jaoui, M., Corse, E., Kleindienst, T.E., Offenberg, J.H., Lewandowski, M., Edney, E.O., 2006. Analysis of secondary organic aerosol compounds from the photooxidation of d-limonene in the presence of NOx and their detection in ambient $PM_{2.5}$. Environ. Sci. Technol. 40 (12), 3819–3828.

Jaoui, M., Edney, E.O., Kleindienst, T.E., Lewandowski, M., Offenberg, J.H., Surratt, J.D., et al., 2008. Formation of secondary organic aerosol from irradiated α-pinene/toluene/NOx mixtures and the effect of isoprene and sulfur dioxide. J. Geophys. Res. Atmos. 113 (D9), D09303.

Jimenez, J.L., Canagaratna, M.R., Donahue, N.M., Prevot, A.S.H., Zhang, Q., Kroll, J.H., et al., 2009. Evolution of organic aerosols in the atmosphere. Science 326 (5959), 1525–1529.

Kampf, C.J., Corrigan, A.L., Johnson, A.M., Song, W., Keronen, P., Königstedt, R.K., et al., 2012. First measurements of reactive α-dicarbonyl concentrations on $PM_{2.5}$ aerosol over the Boreal forest in Finland during HUMPPA-COPEC 2010-source apportionment and links to aerosol aging. Atmos. Chem. Phys. 12 (14), 6145–6155.

Kawamura, K., Yasui, O., 2005. Diurnal changes in the distribution of dicarboxylic acids, ketocarboxylic acids and dicarbonyls in the urban Tokyo atmosphere. Atmos. Environ. 39 (10), 1945–1960.

Kawamura, K., Okuzawa, K., Aggarwal, S.G., Irie, H., Kanaya, Y., Wang, Z., 2013. Determination of gaseous and particulate carbonyls (glycolaldehyde, hydroxyacetone, glyoxal, methylglyoxal, nonanal and decanal) in the atmosphere at Mt. Tai. Atmos. Chem. Phys. 13 (10), 5369–5380.

Kesselmeier, J., Staudt, M., 1999. Biogenic volatile organic compounds (VOC): an overview on emission, physiology and ecology. J. Atmos. Chem. 33 (1), 23–88.

Kirstine, W., Galbally, I., Ye, Y., Hooper, M., 1998. Emissions of volatile organic compounds (primarily oxygenated species) from pasture. J. Geophys. Res. Atmos. 103 (D9), 10605–10619.

Kourtchev, I., Warnke, J., Maenhaut, W., Hoffmann, T., Claeys, M., 2008. Polar organic marker compounds in $PM_{2.5}$ aerosol from a mixed forest site in western Germany. Chemosphere 73 (8), 1308–1314.

Kroll, J.H., Seinfeld, J.H., 2008. Chemistry of secondary organic aerosol: formation and evolution of low-volatility organics in the atmosphere. Atmos. Environ. 42 (16), 3593–3624.

Kuo, S.C., Tsai, Y.I., Tsai, C.H., Hsieh, L.Y., 2011. Carboxylic acids in $PM_{2.5}$ over *Pinus morrisonicola* forest and related photoreaction mechanisms identified via Raman spectroscopy. Atmos. Environ. 45 (37), 6741–6750.

Legrand, M., Preunkert, S., Oliveira, T., Pio, C.A., Hammer, S., Gelencsér, A., et al., 2007. Origin of C_2–C_5 dicarboxylic acids in the European atmosphere inferred from year-round aerosol study conducted at a west–east transect. J. Geophys. Res. Atmos. 112 (D23), D23S07.

Leungsakul, S., Jaoui, M., Kamens, R.M., 2005. Kinetic mechanism for predicting secondary organic aerosol formation from the reaction of d-limonene with ozone. Environ. Sci. Technol. 39 (24), 9583–9594.

Liggio, J., Li, S.M., McLaren, R., 2005. Heterogeneous reactions of glyoxal on particulate matter: identification of acetals and sulfate esters. Environ. Sci. Technol. 39 (6), 1532–1541.

Limbeck, A., Puxbaum, H., Otter, L., Scholes, M.C., 2001. Semivolatile behavior of dicarboxylic acids and other polar organic species at a rural background site (Nylsvley, RSA). Atmos. Environ. 35 (10), 1853–1862.

Matsunaga, S., Mochida, M., Kawamura, K., 2003. Growth of organic aerosols by biogenic semi-volatile carbonyls in the forestal atmosphere. Atmos. Environ. 37 (15), 2045–2050.

Matsunaga, S., Mochida, M., Kawamura, K., 2004. High abundance of gaseous and particulate4-oxopentanal in the forestal atmosphere. Chemosphere 55 (8), 1143–1147.

Matsunaga, S.N., Kato, S.G., Yoshino, A., Greenberg, J.P., Kajii, Y., Guenther, A.B., 2005. Gas-aerosol partitioning of semi volatile carbonyls in polluted atmosphere in Hachioji, Tokyo. Geophys. Res. Lett. 32 (11), L11805.

McClenny, W.A., Daughtrey, E.H., Adams, J.R., Oliver, K.D., Kronmiller, K.G., 1998. Volatile organic compound concentration patterns at the New Hendersonville monitoring

site in the 1995 Southern Oxidants Study in the Nashville, Tennessee, area. J. Geophys. Res. Atmos. 103 (D17), 22509–22518.

Mihalopoulos, N., Stephanou, E., Kanakidou, M., Pilitsidis, S., Bousquet, P., 1997. Tropospheric aerosol ionic composition in the Eastern Mediterranean region. Tellus B 49 (3), 314–326.

Monks, P.S., Granier, C., Fuzzi, S., Stohl, A., Williams, M.L., Akimoto, H., et al., 2009. Atmospheric composition change-global and regional air quality. Atmos. Environ. 43 (33), 5268–5350.

Nannoolal, Y., Rarey, J., Ramjugernath, D., 2008. Estimation of pure component properties: part 3. Estimation of the vapor pressure of non-electrolyte organic compounds via group contributions and group interactions. Fluid Phase Equilib. 269 (1–2), 117–133.

Odum, J.R., Hoffmann, T., Bowman, F., Collins, D., Flagan, R.C., Seinfeld, J.H., 1996. Gas/particle partitioning and secondary organic aerosol yields. Environ. Sci. Technol. 30 (8), 2580–2585.

Pankow, J.F., 1994. An absorption model of the gas/aerosol partitioning involved in the formation of secondary organic aerosol. Atmos. Environ. 28 (2), 189–193.

Putaud, J.P., Van Dingenen, R., Dell'Acqua, A., Raes, F., Matta, E., Decesari, S., et al., 2004. Size-segregated aerosol mass closure and chemical composition in Monte Cimone (I) during MINATROC. Atmos. Chem. Phys. 4 (4), 889–902.

Putaud, J.P., Van Dingenen, R., Alastuey, A., Bauer, H., Birmili, W., Cyrys, J., et al., 2010. A European aerosol phenomenology — 3: physical and chemical characteristics of particulate matter from 60 rural, urban, and kerbside sites across Europe. Atmos. Environ. 44 (10), 1308–1320.

Röhrl, A., Lammel, G., 2002. Determination of malic acid and other C_4 dicarboxylic acids in atmospheric aerosol samples. Chemosphere 46 (8), 1195–1199.

Rolph, G.D., 2014. Real-time environmental applications and display system. (Available at: http://www.ready.noaa.gov. Date accessed: 17 October 2013).

Rossignol, S., Chiappini, L., Perraudin, E., Rio, C., Fable, S., Valorso, R., et al., 2012. Development of parallel sampling and analysis method for the elucidation of gas/particle partitioning of oxygenated semi-volatile organics: a limonene ozonolysis study. Atmos. Meas. Tech. 5 (6), 1459–1489.

Rudich, Y., Donahue, N.M., Mentel, T.F., 2007. Aging of organic aerosol: bridging the gap between laboratory and field studies. Annu. Rev. Phys. Chem. 58 (1), 321–352.

Seinfeld, J.H., Pankow, J.F., 2003. Organic atmospheric particulate material. Annu. Rev. Phys. Chem. 54 (1), 121–140.

Shiraiwa, M., Ammann, M., Koop, T., Pöschl, U., 2011. Gas uptake and chemical aging of semisolid organic aerosol particles. Proc. Natl. Acad. Sci. U. S. A. 108 (27), 11003–11008.

Steitz, B., Gensch, I., Hohaus, T., Saathoff, H., Kiendler-Scharr, A., 2013. Temperature Dependence of Nopinone Partitioning Coefficient in Organic Aerosol. Prague, Czech Republic, European Aerosol Conference.

Temime, B., Healy, R.M., Wenger, J.C., 2007. A denuder-filter sampling technique for the detection of gas and particle phase carbonyl compounds. Environ. Sci. Technol. 41 (18), 6514–6520.

Tsimpidi, A.P., Karydis, V.A., Zavala, M., Lei, W., Molina, L., Ulbrich, I.M., et al., 2010. Evaluation of the volatility basis-set approach for the simulation of organic aerosol formation in the Mexico City metropolitan area. Atmos. Chem. Phys. 10 (2), 525–546.

Valorso, R., Aumont, B., Camredon, M., Raventos-Duran, T., Mouchel-Vallon, C., Ng, N.L., et al., 2011. Explicit modelling of SOA formation from α-pinene photooxidation: sensitivity to vapour pressure estimation. Atmos. Chem. Phys. 11 (14), 6895–6910.

Virtanen, A., Joutsensaari, J., Koop, T., Kannosto, J., Yli-Pirilä, P., Leskinen, J., et al., 2010. An amorphous solid state of biogenic secondary organic aerosol particles. Nature 467 (7317), 824–827.

Wildt, J., Kobel, K., Schuh-Thomas, G., Heiden, A.C., 2003. Emissions of oxygenated volatile organic compounds from plants part II: emissions of saturated aldehydes. J. Atmos. Chem. 45 (2), 173–196.

Worton, D.R., Goldstein, A.H., Farmer, D.K., Docherty, K.S., Jimenez, J.L., Gilman, J.B., et al., 2011. Origins and composition of fine atmospheric carbonaceous aerosol in the Sierra Nevada Mountains, California. Atmos. Chem. Phys. 11 (19), 10219–10241.

Zhang, H., Surratt, J.D., Lin, Y.H., Bapat, J., Kamens, R.M., 2011. Effect of relative humidity on SOA formation from isoprene/NO photooxidation: enhancement of 2-methylglyceric acid and its corresponding oligoesters under dry conditions. Atmos. Chem. Phys. 11 (13), 6411–6424.

Zheng, M., Cass, G.R., Schauer, J.J., Edgerton, E.S., 2002. Source apportionment of $PM_{2.5}$ in the Southeastern United States using solvent-extractable organic compounds as tracers. Environ. Sci. Technol. 36 (11), 2361–2371.